New Phytologist

Research

Ectopic expression of Kip-related proteins restrains root-knot nematode-feeding site expansion

Paulo Vieira[1]*, Carmen Escudero[1], Natalia Rodiuc[1], Joanna Boruc[2,3†], Eugenia Russinova[2,3], Nathalie Glab[4], Manuel Mota[5], Lieven De Veylder[2,3], Pierre Abad[1], Gilbert Engler[1] and Janice de Almeida Engler[1]

[1]Institut National de la Recherche Agronomique, UMR 1355 ISA/Centre National de la Recherche Scientifique, UMR 7254 ISA/Université de Nice-Sophia Antipolis, UMR ISA, 400 route des Chappes, Sophia-Antipolis, France; [2]Department of Plant Systems Biology, VIB, B-9052, Gent, Belgium; [3]Department of Plant Biotechnology and Bioinformatics, Ghent University, B-9052, Gent, Belgium; [4]UMR8618, CNRS Université Paris-Sud 11, Bat 630, 91405, Orsay, France; [5]NemaLab/ICAAM – Instituto de Ciências Agrárias e Ambientais Mediterrânicas, Universidade de Évora, Núcleo da Mitra, Ap. 94, 7002-554, Évora, Portugal; *Present address: NemaLab/ICAAM - Instituto de Ciências Agrárias e Ambientais Mediterrânicas, Universidade de Évora, Núcleo da Mitra, Ap. 94, 7002-554, Évora, Portugal; †Present address: Department of Molecular Genetics, The Ohio State University, OH 43210, USA

Author for correspondence:
Janice de Almeida Engler
Tel: +33 492 386 459
Email: janice.almeida-engler@sophia.inra.fr

Received: *24 January 2013*
Accepted: *1 March 2013*

New Phytologist (2013)
doi: 10.1111/nph.12255

Key words: Arabidopsis roots, cell cycle, giant cells, *Meloidogyne*, nuclei.

Summary

• The development of nematode feeding sites induced by root-knot nematodes involves the synchronized activation of cell cycle processes such as acytokinetic mitoses and DNA amplification. A number of key cell cycle genes are reported to be critical for nematode feeding site development. However, it remains unknown whether plant cyclin-dependent kinase (CDK) inhibitors such as the Arabidopsis interactor/inhibitor of CDK (ICK)/Kip-related protein (KRP) family are involved in nematode feeding site development. This study demonstrates the involvement of Arabidopsis ICK2/KRP2 and ICK1/KRP1 in the control of mitosis to endoreduplication in galls induced by the root-knot nematode *Meloidogyne incognita*.

• Using *ICK/KRP* promoter-GUS fusions and mRNA *in situ* hybridizations, we showed that *ICK2/KRP2*, *ICK3/KRP5* and *ICK4/KRP6* are expressed in galls after nematode infection. Loss-of-function mutants have minor effects on gall development and nematode reproduction. Conversely, overexpression of both *ICK1/KRP1* and *ICK2/KRP2* impaired mitosis in giant cells and blocked neighboring cell proliferation, resulting in a drastic reduction of gall size.

• Studying the dynamics of protein expression demonstrated that protein levels of ICK2/KRP2 are tightly regulated during giant cell development and reliant on the presence of the nematode.

• This work demonstrates that impeding cell cycle progression by means of *ICK1/KRP1* and *ICK2/KRP2* overexpression severely restricts gall development, leading to a marked limitation of root-knot nematode development and reduced numbers of offspring.

Introduction

Plant-parasitic nematodes belonging to the genus *Meloidogyne* are one of the most important obligate parasites infecting a wide range of cultivated plants. World-wide, they are responsible for billions of dollars in crop losses annually. *Meloidogyne* species, or root-knot nematodes (RKNs), are capable of inducing the formation of feeding sites within the vascular tissue, containing five to eight hypertrophied giant cells (GCs). Nematode feeding sites (NFSs), or galls, contain GCs that function as carbon sinks, have been depicted as transfer cells and serve as the sole source of nutrition for the nematode (Jones & Northcote, 1972; Caillaud *et al.*, 2008). GCs undergo multiple rounds of nuclear division without cytokinesis. Concomitant with GC development, neighboring cells recurrently divide asymmetrically and support the transfer of nutrients to these feeding cells (Jones & Northcote, 1972; Wiggers *et al.*, 1990; Hoth *et al.*, 2008). As GCs develop, their nuclei undergo multiple rounds of DNA synthesis, coupled with an increase in cell size. Hyperplasia of neighboring cells and hypertrophy of GCs produce the typical root-knot or gall enclosing the nematode (Jones & Northcote, 1972).

Development of the NFS relies on a continuous molecular dialogue between the nematode and the host plant. Among the primary events occurring during NFS formation, cell cycle gene activation is a crucial process leading to multiple mitotic events in both GCs and neighboring cells (de Almeida Engler *et al.*, 1999, 2011; Gheysen & Fenoll, 2002). Intensive DNA replication probably results in increased ploidy levels, consequently triggering GC expansion. To date, a number of core cell cycle genes positively controlling the cell cycle have been shown to be crucial for NFS formation (de Almeida Engler *et al.*, 1999, 2011, 2012). Two cyclin-dependent kinases (*CDKA;1* and *CDKB1;1*) and two mitotic cyclins (*CYCB1;1* and *CYCA2;1*) are induced early in Arabidopsis galls, indicating that host cell cycle gene activation is important for NFS establishment (Niebel *et al.*, 1996; de Almeida Engler *et al.*, 1999, 2011). Other key regulators of the cell cycle,

such as the endocycle activators CCS52A and CCS52B (CCS, cell cycle switch) or the inhibitor of endoreduplication E2Fe/DEL1 (E2F-like proteins), have been shown to be key components of the endocycle in nematode-induced feeding sites (de Almeida Engler *et al.*, 2012). Disruption of NFS development occurs when treatment of infected roots with chemical cell cycle phase-specific blockers (e.g. hydroxyurea and oryzalin) results in reduced nematode reproduction (de Almeida Engler *et al.*, 1999, 2011). Van de Capelle *et al.* (2008) have shown that *AtCDKA;1* knockdown also interferes with NFS development, resulting in decreased nematode reproduction.

The mechanisms that regulate the cell cycle in plants involve multiple core components. Progression through the cell cycle is strictly regulated by the activation of cyclin-dependent kinases (CDKs), and monitored by the concerted action of at least four classes of regulatory protein complexes, including positive regulators (cyclins), negative regulators (CDK inhibitors) and activating or inhibitory kinases (CAK (CDK-activating kinases) and WEE1 (WEE1 kinase gene), respectively; Van Leene *et al.*, 2010a). CDKA;1 has been implicated in both G1-to-S and G2-to-M transitions and associates with D-type cyclins (CYCDs), while CDKB kinases control the G2-to-M transition (Inzé & De Veylder, 2006). The switch from the mitotic cell cycle to the endocycle usually involves the downregulation of CDK/CYC activity to skip mitosis while permitting DNA replication (De Veylder *et al.*, 2011). However, the mitotic and endoreduplication cycles share many of their key regulators, such as the S-phase cyclins and CDKs, which are essential for progression through the endoreduplication cycle (Joubès & Chevalier, 2000; Edgar & Orr-Weaver, 2001).

CDK activity is controlled by CDK inhibitors (CKIs), which in turn are negatively regulated through degradation by SCF (Skp1, Cullins, F-box proteins)-type ubiquitin E3 ligases (Inzé & De Veylder, 2006). Plant genomes encode two plant-specific families of CKIs, the interactor/inhibitor of CDK/Kip-related protein (ICK/KRP) and SIM/SMR (SIAMESE/SIAMESE-related) families (Wang *et al.*, 1997; De Veylder *et al.*, 2001; Churchman *et al.*, 2006; Peres *et al.*, 2007). The ICK/KRP cell cycle inhibitors were initially described for Arabidopsis, but were later also identified in other plant species such as rice (*Oryza sativa*; Barrôco *et al.*, 2006), maize (*Zea mays*; Coelho *et al.*, 2005), tobacco (*Nicotiana tabacum*; Jasinski *et al.*, 2002), tomato (*Solanum lycopersicum*) (Bisbis *et al.*, 2006) and alfalfa (*Medicago sativa*) (Pettko-Szandtner *et al.*, 2006). In Arabidopsis, seven *ICK/KRP* gene family members have been identified, and all their encoded proteins localized to the nucleus (De Veylder *et al.*, 2001; Bird *et al.*, 2007; Wang *et al.*, 2008; Boruc *et al.*, 2010a). At the tissue and cellular levels, transcript patterns of all Arabidopsis *ICK/KRP* genes have been reported (Ormenese *et al.*, 2004; de Almeida Engler *et al.*, 2009). Also, the fine-tuning of ICK/KRP protein abundance is a key factor in maintaining the balance between cell proliferation and cell differentiation (Verkest *et al.*, 2005a; Weinl *et al.*, 2005). High overexpression of *ICK/KRP* genes has particular effects on plant morphology and cellular differentiation, while moderate overexpression of *ICK/KRP* genes favors endoreduplication over mitotic cell division. In the latter case, only minor alterations were observed in cell size, with a slight decrease in final plant size (Verkest *et al.*, 2005b; Weinl *et al.*, 2005). However, higher levels of ICK/KRP negatively affect both cell division and endoreduplication, resulting in enlarged cells (e.g. in leaves) and altered plant morphogenesis, such as a serrated leaf phenotype (Wang *et al.*, 2000; De Veylder *et al.*, 2001; Jasinski *et al.*, 2002; Zhou *et al.*, 2002; Barrôco *et al.*, 2006; Bemis & Torii, 2007; Kang *et al.*, 2007).

Development of the NFS during RKN parasitism seems to require the involvement and regulation of both the mitotic and endoreduplication cycles. Endoreduplication is characterized by the occurrence of repetitive cycles of DNA replication in cells that do not enter mitosis. Consequently, repeated endocycle rounds will lead to duplicated chromatids that remain associated within a single chromocenter. Differently, duplication of chromosomes during endomitosis occurs in cells that can enter mitosis but fail to complete telophase and/or cytokinesis, often leading to an increase in chromosome number (Comai, 2005). The precise mechanisms by which RKNs manipulate both cell cycle programs, including the mechanism of cytokinesis disruption, remain to be elucidated. Here we report on the potential involvement of members of the Arabidopsis ICK/KRP (hereafter KRP) family in NFS ontogeny. Three *KRP* genes (*KRP2*, *KRP5* and *KRP6*) are highly expressed in gall tissues, suggesting their involvement in cell cycle control of NFS development in Arabidopsis. We showed by functional analysis that KRP loss-of-function mutants ($krp2^{-/-}$, $krp2^{-/-}krp6^{-/-}$ and *krp*∅; see Materials and Methods for mutant definitions) were not affected in gall development or nematode reproduction. In contrast, ectopic *KRP* expression resulted in reduced mitosis and changes in ploidy levels, which prevented cells from undergoing the endocycle in GCs. Overexpression of two Arabidopsis *KRP*s had a profound effect on GC expansion and neighboring cell division, severely reducing gall size, and thereby significantly inhibiting nematode development and reproduction.

Materials and Methods

Plant growth conditions and transformations

Arabidopsis thaliana (L.) Heynh. genotype Columbia (Col-0) was used as the wild-type control. For construction of the *KRPpro:GUS* (*KRP1* to *KRP7*) lines, the intergenic regions (up to a maximum of 2 kp) were amplified from Arabidopsis genomic DNA. The corresponding PCR fragments were cloned into the pDONR207 entry vector by BP (BP clonase; Gateway system) recombination cloning and subsequently transferred into the pKGWFS7 destination vector (Karimi *et al.*, 2002) by LR (LR clonase; Gateway system) cloning, resulting in a transcriptional fusion between the *KRP* promoters and the *EGFP-GUS* fusion gene. The *KRP2* single T-DNA insertion mutant line (SALK_130744) was obtained from the Arabidopsis Biological Resource Center. The $krp2^{-/-}krp6^{-/-}$ mutant line was obtained by crossing the *KRP2* and *KRP6* single T-DNA insertion lines (SALK_069817 and SAIL_54B_B03, respectively). A multiple-silencing *KRP* line (line 2.7 from Anzola *et al.* (2010), hereafter

referred to as *krp∅*) was kindly provided by C. Luschnig (Department of Applied Genetics and Cell Biology, BOKU, Vienna, Austria). Homozygous knockout mutant lines (*krp2* and *krp2*$^{-/-}$ *krp6*$^{-/-}$) were tested by PCR with specific primers using genomic DNA (Supporting Information Table S1). Kanamycin-resistant T3 overexpression lines (*35S:KRP1-GFP* and *35S:GFP-KRP2*, hereafter referred to as *KRP1*^{OE} and *KRP2*^{OE}, respectively) were evaluated based on *KRP* expression levels, protein localization and plant phenotype. Seeds from Arabidopsis transgenic lines and wild-type Col-0 were surface-sterilized for 10 min in 5% NaOCl, followed by four washes with 95% ethanol, and dried overnight. Seeds were kept in a growth chamber with a 16 h light : 8 h dark photoperiod at 21 : 18°C, respectively.

Histochemical GUS assay and microscopy analysis

The promoter activity of the seven *KRP* Arabidopsis genes was monitored at 7, 14, and 21 d after inoculation (DAI), as described by de Almeida Engler *et al.* (1999). Two incubation periods (3 and 24 h) were applied to gall samples to better evaluate GUS activity for each *KRP*$_{pro}$*:GUS* line. To prevent diffusion of the GUS precipitate, galls were fixed in 2.0% glutaraldehyde overnight and were embedded in Technovit 7100 (Heraeus Kulzer, Wehrheim, Germany), sectioned (3 μm), and microscopically analyzed using dark-field optics. Otherwise, seedlings and galls were fixed and transferred to a chlorallactophenol-clearing solution (Beeckman & Engler, 1994) for observation using Normasky optics.

mRNA *in situ* hybridization

Fixation, embedding and sectioning were performed on galls at 14 DAI. Samples were degassed under vacuum in fixative (2.5% glutaraldehyde) and incubated in fresh fixative under rotation at 4°C for at least 1 wk, with the fixative being replaced with fresh fixative every 2 d. Dissection and fixation of feeding sites, gene-specific sense and antisense probes of the seven Arabidopsis *KRP* genes, and the *in situ* hybridization procedure were as described by de Almeida Engler *et al.* (2009). Seventy microliters of 15×10^6 c.p.m. was applied per slide (7.5 ng per slide). After exposure at 4°C in dry boxes in absolute darkness, slides were developed, fixed and stained with 0.05% toluidine blue. Images were taken with an Axiocam digital camera (Zeiss, Jena, Germany) with standard dark-field optics.

RNA isolation and RT-PCR analyses of *KRP* knockout and overexpressing lines

Total RNA was extracted with Trizol reagent (Invitrogen, Paisley, UK) from 7-d-old whole seedlings, using the RNeasy Plant Mini Kit (Qiagen) according to the manufacturer's instructions. The RNA was treated with RQ1 RNase-free DNase (Promega) before reverse transcription. One microgram of treated RNA was added to RT reactions using a Bio-Rad iScript first-strand synthesis kit with random hexamer primers to make cDNA. Semiquantitative RT-PCR amplification was performed with specific primer pairs (Table S1).

Morphological analysis

Surface-sterilized seeds of Arabidopsis Col-0 and transgenic lines were germinated, and infected as described by de Almeida Engler *et al.* (1999). Seeds were placed in sterile Petri dishes on 1% Murashige and Skoog (MS) germination medium (Duchefa, Haarlem, the Netherlands) containing 1% sucrose and 0.8% plant cell culture-tested agar (Sigma-Aldrich), supplemented with the appropriate antibiotics. Plantlets were grown vertically, to allow roots to grow at the surface, with a 16 h light : 8 h darkness photoperiod at 21 : 18°C, respectively. Roots of T3 lines were infected, collected at 7, 14, 21 and 40 DAI and fixed in 2% glutaraldehyde in 50 mM PIPES buffer, pH 6.9, and then dehydrated and embedded in Technovit 7100 (Heraeus Kulzer) as described by the manufacturer. Embedded roots and gall tissues were sectioned (3 μm), stained in 0.05% toluidine blue and mounted in Depex (Sigma-Aldrich). Microscopic observations were performed using bright-field optics and images were obtained with a digital camera (Axiocam; Zeiss).

Giant cell and nucleus surface measurements

Two to three of the largest GCs per gall section were selected and analyzed at different time-points after nematode infection (7, 14, 21 and 40 DAI) and the surface was measured using the AxioVisionLE (Zeiss) software. A minimum of 60 GCs were measured, from root sections, for each time-point studied. For the GC nucleus surface, a minimum of 80 nuclei were measured at 7, 14 and 21 DAI per mutant at each time-point. The effects of mutant and time were analyzed using two-way analysis of variance (ANOVA) with interaction. Significant differences between average values were identified by means of a Tukey–Kramer test. All computations were carried out with PROC GLM in SAS (version 9.1.3; SAS Institute Inc., Cary, NC, USA).

Nematode infection tests

Three-week-old Arabidopsis Col-0 and transgenic seedlings were transferred to MS medium in Petri dishes, with five plants per plate and six replica plates per line. One root tip from each plant was inoculated with *c.* 100 surface-sterilized, freshly hatched second-stage juveniles (J2s) of *Meloidogyne incognita*, as previously described (de Almeida Engler *et al.*, 1999, 2011). Six to seven weeks after infection, the numbers of galls and egg masses were counted on each plate and compared with those for the control plants. All infection tests were performed for two independent biological experiments, and for each transgenic line.

Flow cytometry analyses

Plant roots were chopped with a razor blade in 400 μl of 45 mM $MgCl_2$, 30 mM sodium citrate, 20 mM 3-(N-morpholino)

propanesulfonic acid, pH 7, and 0.1% Triton X-100 (Galbraith *et al.*, 1991). The supernatant was filtered over a 30-mm mesh, and 1 μl of 4,6-diamidino-2-phenylindole (DAPI) from a stock of 1 mg ml^{-1} was added. The nuclei were analyzed with the LSRII Fortessa (BD Biosciences, San Jose, CA, USA) flow cytometer and the BD FACSDiva software (BD Biosciences). For uninfected and gall-less roots, data were collected from *c.* 2000 nuclei per run. Three independent biological repetitions were performed using roots of six plants for each line and each analysis. Ploidy levels of 30 galls (40 DAI) were pooled for each independent experiment. Two replicates and two biological repetitions were performed for each line, and data for *c.* 40 000 nuclei per run were collected. The mean values of repetitions of independent experiments were calculated, and the fraction of nuclei with ploidy levels from 2C to 64C was expressed as the percentage of the total number of nuclei measured.

In vivo observation of BY-2 tobacco cells and fresh gall root slices and whole roots

Transformation of cells of *Nicotiana tabacum* L. cv bright yellow 2 (BY-2) was carried out as described by Geelen & Inzé (2001). Observation of the nuclei in noninfected and infected material from wild-type and transgenic lines was performed in Arabidopsis seedlings harboring free GFP (*35S:GFP*) and *KRP* overexpressing lines. Galls at various time-points after infection (7–40 DAI) were dissected from roots and embedded in 5% agar. Fresh thick sections of 50–100 μm (7–14 DAI) or 150–200 μm (14–40 DAI) were cut with an Microm HM650V Vibratome (Walldorf, Germany). Whole roots and fresh slices were observed using an inverted confocal microscope (model LSM510 META; Zeiss). GFP was excited with a 488 nm Argon laser and fluorescence was captured in lambda mode using a 499–550 nm bandwith. All observations were performed in at least three independent experiments.

Electron microscopy of galls

Root galls of Arabidopsis Col-0 and $KRP2^{OE}$ were dissected at 30 DAI and fixed in a mixture of 1.5% glutaraldehyde and 3% paraformaldehyde in 10 mM phosphate-buffered saline (PBS) containing 150 mM NaCl (pH 7.2) for 3 h at room temperature. After several washes in PBS, fixed galls were incubated in 0.5 M NH_4Cl for 1 h, dehydrated in a graded ethanol series, embedded in LR White acrylic resin (Sigma), and polymerized overnight at 60°C. Ultrathin sections were collected on parlodion-coated nickel grids, treated with 0.1 M HCl for 10 min, and washed at least twice with double-distilled water. Samples were observed under a Philips 400T electron microscope.

Whole-mount analysis of propidium iodide-stained and cleared nuclei

Nuclear analysis of cleared NFSs was performed based on the protocol described by Vieira *et al.* (2012), for uninfected roots and nematode-infected roots (7–40 DAI). Propidium iodide (PI)-stained samples were mounted with 90% glicerol on a slide. Cleared samples were analyzed with a Zeiss LSM 510 META confocal microscope. Dye excitation was performed with the 543-nm line of a HeNe laser. Stacks were generated from *c.* 50 images of 1 μm optical slice thickness and represented as maximum brightness projections.

Acid fuchsin nematode staining

Infected roots at 40 DAI were fixed and stained for 5 h in a solution of equal parts of 95% ethanol and glacial acetic acid, containing 17.5 mg l^{-1} acid fuchsin. Root tissues were de-stained by soaking in a solution of chloral hydrate (0.2 g ml^{-1} of H_2O) for 16 h. After rinsing several times with tap water, roots containing nematodes were stored in acidified glycerol (five drops of 1.0 M HCl in 50 ml of glycerol).

Results

Expression of *KRP* genes in galls

The promoter activity of all members of the *KRP* family was monitored by performing GUS assays at different stages of gall development (early, 7 DAI; intermediate, 14 DAI; and late, 21 DAI) on Arabidopsis roots. To determine the expression pattern of *KRP* genes in roots, the promoter activity was examined before nematode infection (Fig. S1). GUS staining performed on entire galls revealed high promoter activity of the *KRP2*, *KRP5* and *KRP6* genes during all stages of gall development (Fig. S2, Table S2). By contrast, all other *KRP* family members (*KRP1*, *KRP3*, *KRP4* and *KRP7*) showed no GUS activity at comparable time-points during gall development (Figs S2, S3, Table S2). Tissue sections of galls showed the precise localization of promoter activity of the *KRP2*, *KRP5* and *KRP6* genes at the different developmental stages (Fig. 1a). At 7 DAI, both GCs and neighboring cells revealed high GUS staining for the three *KRP* genes (Fig. 1a) concomitant with the high mitotic activity in galls. At 14 DAI, *KRP2* revealed a stronger promoter activity in GCs than *KRP5* and *KRP6* (Fig. 1a). *KRP6* expression was higher in neighboring cells during gall development (7–14 DAI). A general decrease in GUS activity was observed in galls of 21 DAI for the three *KRP*s (Fig. 1a), in comparison to the other time-points studied. Transcript localization was verified by *in situ* hybridization, and the expression patterns of the seven *KRP* genes were coherent with the promoter activities measured by GUS assays (Figs 1b, S4).

Loss of *KRP2* function induces mitosis in galls

To address whether a loss of function of an actively transcribed *KRP* in galls could disrupt NFS and nematode development, we used single insertion mutant lines (*krp2*). Anticipating a possible redundancy of function among the different *KRP* genes, we further analyzed one double mutant ($krp2^{-/-}$ $krp6^{-/-}$) and a multi-*krp* silencing line for the seven genes (*krp∅*; Fig. S5). To assess the effect of loss of *KRP* function during NFS development (7, 14 and 21 DAI), a detailed morphological analysis was performed.

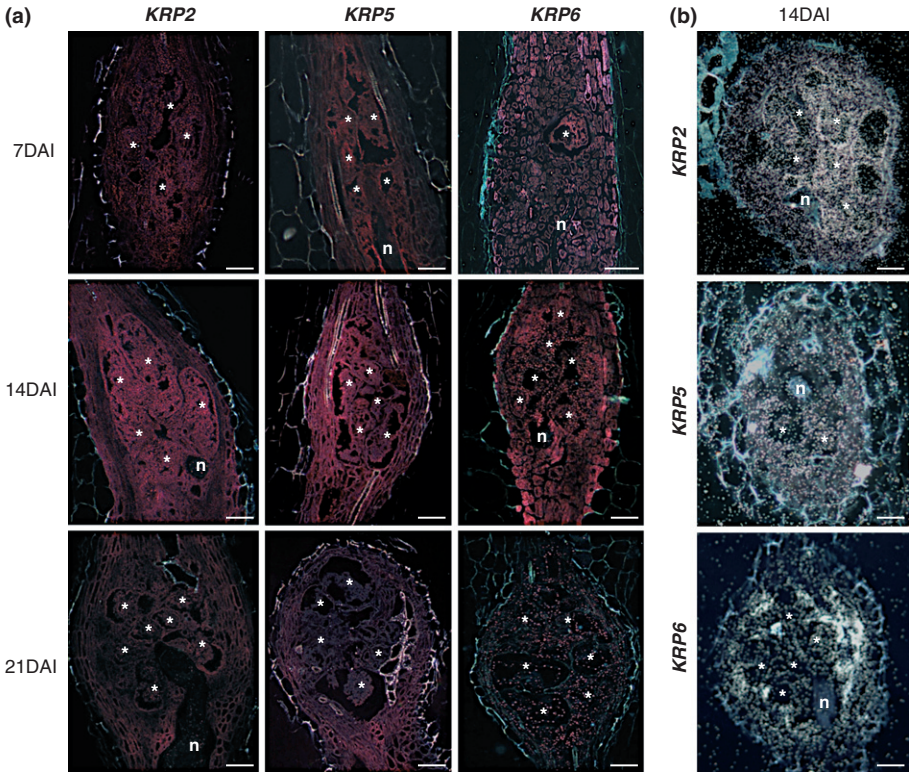

Fig. 1 Expression patterns for three *KRPpro:GUS* Arabidopsis lines in galls of roots infected with *Meloidogyne incognita*. (a) Promoter activity of Kip-related protein 2 (*KRP2*), *KRP5* and *KRP6* during gall development (7, 14 and 21 d after inoculation (DAI)). Dark-field images illustrate GUS staining in red. (b) mRNA *in situ* localization in galls 14 DAI. Sections were hybridized with 35S-labeled antisense RNA probes. The hybridization signal is presented as white dots under dark-field optics. Asterisk, giant cell; n, nematode. Bars, 50 μm.

Although the overall morphology of galls induced in mutant lines was apparently similar to that of the wild type, unusual proliferation of neighboring cells was observed in both *krp2* and $krp2^{-/-}\,krp6^{-/-}$ mutants (obvious at 14 and 21 DAI in Fig. 2). Mitotic figures, rarely seen in wild-type Arabidopsis GCs, were ubiquitous in the *krp2* line (Fig. S6). Increased numbers of GC nuclei were obvious in the *krp2* mutant, the $krp2^{-/-}\,krp6^{-/-}$ double mutant and the *krp∅* line (Figs 2, 3a) compared with the wild type (Fig. 3b). Nematode infection tests were performed to examine whether these mutants (except for *krp∅*) had any effect on nematode development and reproductive ability. No significant changes in gall size or in egg mass number could be observed (Fig. S7).

Overexpression of *KRP* genes affects gall development

The effect of the overexpression of *KRP* genes during NFS development was investigated for two *KRP* genes; *KRP2*, which is highly expressed in galls, and *KRP1*, which is not expressed in galls. This resulted in the generation of several overexpressing transgenic lines for the *KRP1* and *KRP2* genes. Lines selected for RKN infection were based on the serrated leaf phenotype (Fig. S8a), and to assure increased expression levels RT-PCR analysis was performed (Fig. S8b). Constructs were also validated based on the expected nuclear localization of KRP proteins (Fig. S8c). Additional phenotypes for both overexpression lines, such as undersized root apical meristems, were microscopically analyzed (Fig. S8d). To evaluate the effects of ectopic *KRP1* and *KRP2* expression on NFS ontogeny, a detailed microscopic analysis was performed at different stages of gall development (7, 14, 21 and 40 DAI). We observed that ectopic *KRP1* and *KRP2* expression severely reduced the division of cells neighboring GCs as compared with the wild-type gall (Fig. 4). In addition, GCs within roots of the $KRP1^{OE}$ and $KRP2^{OE}$ lines appeared smaller than in infected wild-type plants. Surface measurements were carried out on a minimum of 60 GCs per KRP^{OE} line at 7, 14, 21 and 40 DAI, and compared with the size of wild-type GCs (Fig. 5). The average surface of GCs in the $KRP1^{OE}$ (after 14 DAI) and $KRP2^{OE}$ lines was smaller than that of wild-type GCs (Fig. 5a,b). Statistical analysis revealed that the average size of maturing GCs in both overexpressing lines was significantly smaller than the corresponding average size obtained from measurements on wild-type GCs (Fig. 5b). Neighboring cells in galls overexpressing either *KRP1* or *KRP2* were elongated and vacuolated, like uninfected vascular root cells. By contrast, neighboring cells in wild-type galls were small, showed irregular shapes and contained a dense cytoplasm indicative of active cell division.

KRP overexpression induces nuclear changes in giant cells

Analyses carried out on nuclei of GCs of both KRP^{OE} lines showed that their size and number were highly variable within GCs at different developmental stages. Therefore, gall sections of $KRP1^{OE}$ and $KRP2^{OE}$ lines were stained with DAPI and were found to exhibit fewer nuclei, suggesting a reduction in nuclear division compared with wild type (Fig. 6a). These observations were confirmed by electron microscopy analysis (Fig. S9). Nuclear surfaces of GC sections were then measured for the $KRP1^{OE}$ and $KRP2^{OE}$ lines, and compared with the size of wild-type GC nuclei (Fig. 6b,c) at different phases of gall development

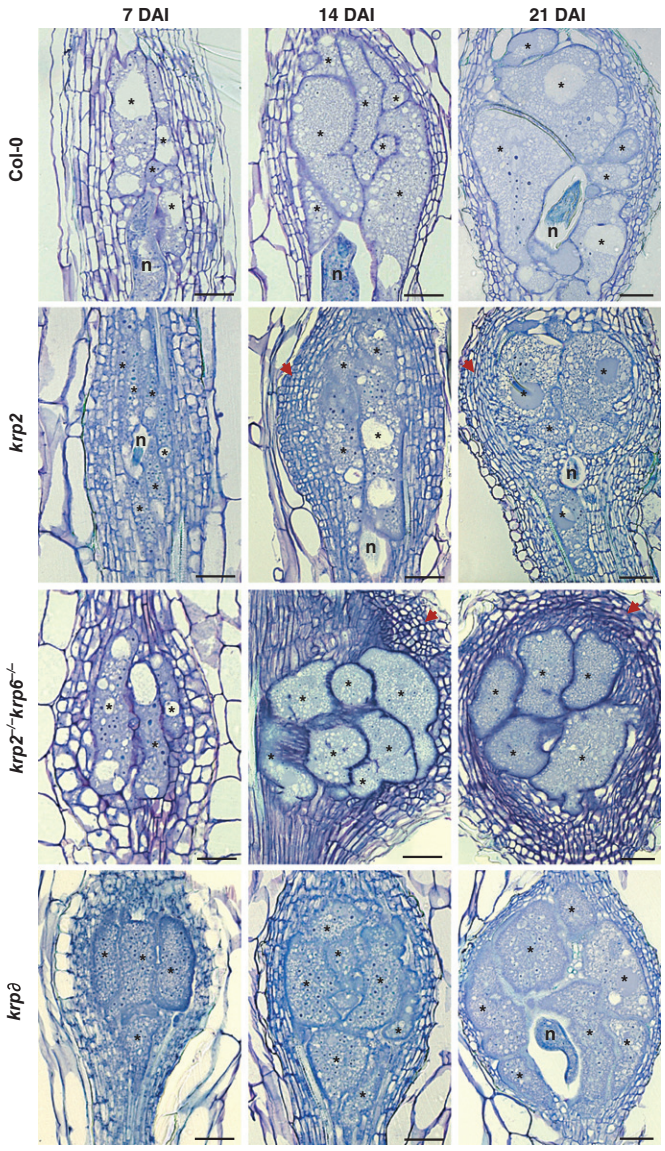

Fig. 2 Histological analysis of gall tissues in Kip-related protein (*krp*) knockout lines of Arabidopsis upon infection with *Meloidogyne incognita*. Bright-field images of longitudinal sections of galls stained with toluidine blue in wild type and *krp2*, *krp2*$^{-/-}$*krp6*$^{-/-}$ and *krp*∂ mutants at different stages of nematode infection (7, 14 and 21 d after inoculation (DAI)) are shown. In the *krp2*, *krp2*$^{-/-}$*krp6*$^{-/-}$ and *krp*∂ mutant lines, a significant increase in the number of nuclei in giant cells is observed. In the *krp2* and *krp2*$^{-/-}$*krp6*$^{-/-}$ lines (arrows), we also observe an elevated proliferation of cells neighboring giant cells compared with a wild-type gall. Asterisk, giant cell; n, nematode. Bars, 50 μm.

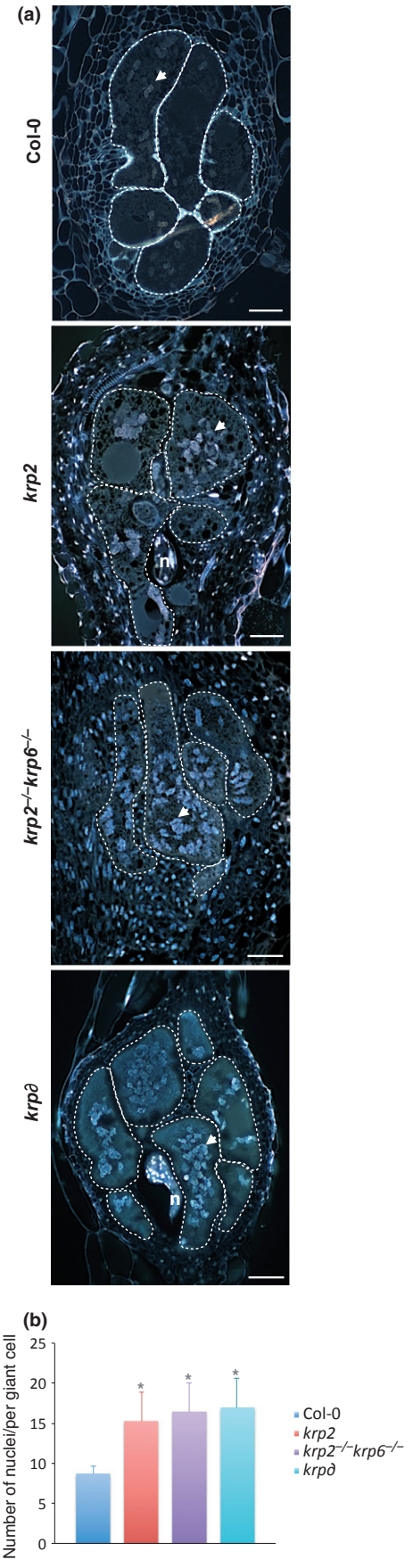

Fig. 3 Loss of Kip-related protein (*krp*) function affects mitosis in giant cells. (a) 4,6-Diamidino-2-phenylindole (DAPI)-stained gall sections at 21 d after inoculation (DAI) of the wild type and the *krp2*, *krp2*$^{-/-}$*krp6*$^{-/-}$ and *krp*∂ mutant lines, respectively. In the *krp2*, *krp2*$^{-/-}$*krp6*$^{-/-}$ and *krp*∂ mutant lines, a significant increase in the number of nuclei is observed. White circles delimit giant cells. Arrows indicate different numbers of nuclei within a single giant cell, as an example. Bars, 50 μm. (b) Average number of nuclei per giant cell at 14 DAI. These values are representative of the number of nuclei per giant cell section. The nuclei were counted in the largest giant cells (two to three) in each gall, using 20 galls for each line. Error bars represent standard deviation and asterisks indicate values that are significantly different from wild-type (Student's *t*-test, $P < 0.05$).

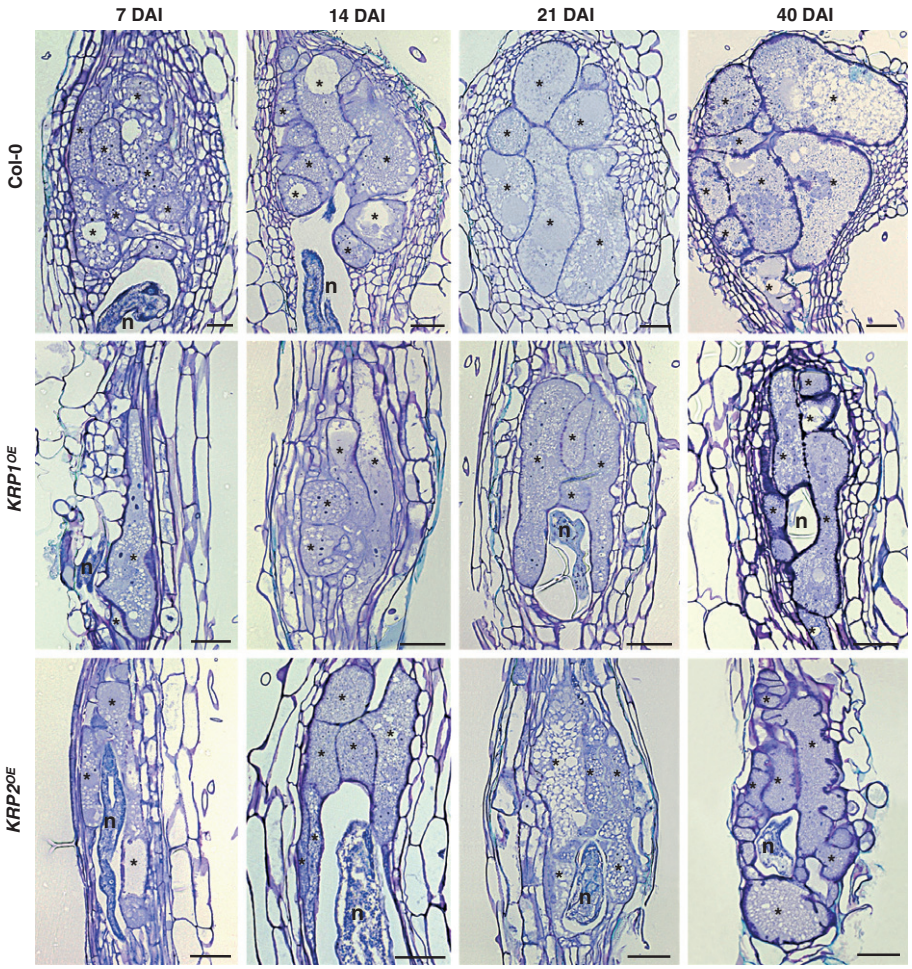

Fig. 4 Ectopic Kip-related protein (*KRP*) expression drastically affects the size of galls induced by *Meloidogyne incognita*. Histological analysis of wild-type galls compared with *KRP1*^{OE} and *KRP2*^{OE} lines at different stages of nematode infection (7, 14, 21 and 40 d after inoculation (DAI)) was performed. Bright-field images of longitudinal gall sections stained with toluidine blue are shown. Note that ectopic *KRP1* and *KRP2* expression drastically reduced the number of nuclei within the giant cells and neighboring cell division (with these cells being larger than wild type). Giant cells were also smaller in the *KRP1*^{OE} and *KRP2*^{OE} lines. Asterisk, giant cell; n, nematode. Bars, 50 μm.

(7, 14 and 21 DAI). As a consequence of the complex and convoluted shape of the nuclei that clustered in GCs at the latest timepoint (40 DAI), similar measurements were not performed. The graph in Fig. 6(b) illustrates that a positive correlation was observed between GC nuclear size and gall development, suggesting that the nuclei of all lines tested undergo gradual DNA amplification (Fig. 6b). Although fewer nuclei were present in the *KRP1*^{OE} line compared with the wild type, we observed a faster increase in nuclear size compared with *KRP2*^{OE} or wild type (Fig. 6b,c). This suggests that these nuclei may enter the endoreduplication cycle earlier. Conversely, in *KRP2*^{OE} infected roots, most GC nuclei presented a smaller surface compared with the wild type, suggesting an inhibition of the endoreduplication cycle (Fig. 6b,c).

We further studied the nuclear distribution and morphology in galls by confocal imaging of cleared and PI-stained galls (Fig. 7). Three-dimensional confocal projections of serial optical sections of galls at 7, 21 and 40 DAI in the *KRP*^{OE} line were generated, and compared with those for the wild type (Fig. 7a–c; Movie S1a). GCs in *KRP1*^{OE} presented fewer and larger nuclei (Fig. 7d–e; Movie S2a), while GCs in the *KRP2*^{OE} line displayed fewer but generally smaller nuclei (Fig. 7g–h; Movie S3a). Densely stained heterochromatic regions, possibly corresponding to chromocenters, were visible as strong brighter spots. Nuclei of uninfected root cells revealed the typical 10 chromocenter-like spots (Fig. 7c′), while several GC nuclei (at 40 DAI) of the wild type (Fig. 7c; Movie S1b), the *KRP1*^{OE} line (Fig. 7f; Movie S2b) and the *KRP2*^{OE} line (Fig. 7i; Movie S3b) were filled with > 20 densely PI-stained heterochromatin foci of different sizes and fluorescence intensities.

Ectopic *KRP* expression induces changes in ploidy levels in gall cells

In order to determine and compare ploidy levels in wild-type and *KRP*^{OE} galls, flow cytometry measurements were conducted. DNA ploidy levels of uninfected wild-type roots and gall-less infected Arabidopsis roots overexpressing *KRP*s (40 DAI) were measured as controls. Nuclear flow cytometry analyses revealed that the ploidy levels of uninfected roots and gall-less infected roots of the wild type and mutant lines ranged from 2C to 16C (Figs 8a,b, S10). Ploidy populations of nuclei in *KRP1*^{OE} and *KRP2*^{OE} galls, compared with the wild type, were measured on a pool of 30 mature galls (per sample) per line at 40 DAI. Ploidy levels for wild-type galls ranged from 2C to 64C (Fig. 8c,d), where > 50% of the nuclei showed 2C DNA content, probably

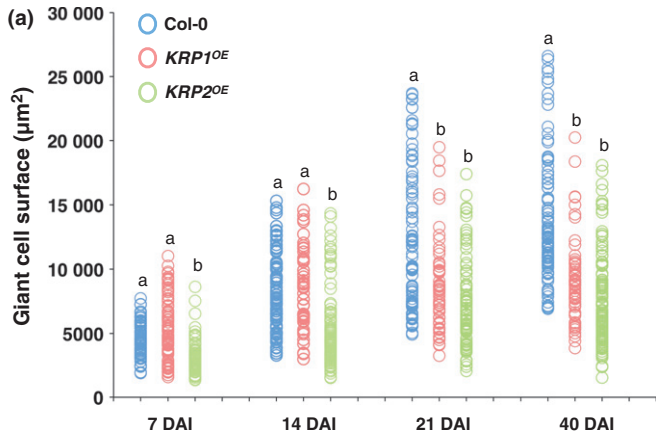

(b)

SURFACE		Col-0	$KRP1^{OE}$	$KRP2^{OE}$
	TIME	7DAI	14DAI	21DAI
Col-0	7DAI		0.0057	<0.0001
$KRP1^{OE}$	14DAI	<0.0001		<0.0001
$KRP2^{OE}$	21DAI	<0.0001	<0.0001	

Fig. 5 Ectopic Kip-related protein (*KRP*) expression reduces giant cell expansion. (a) The giant cell surface (μm^2) in wild-type plants and the $KRP1^{OE}$ and $KRP2^{OE}$ lines was measured at different stages of nematode infection (7, 14, 21 and 40 d after inoculation (DAI)). Measurements were made on a minimum of 60 giant cell sections (only the two to three largest giant cells were measured per gall). Different letters indicate statistically significant differences at each time-point after nematode infection ($P < 0.0001$). (b) Multiple overall comparisons of giant cell surface development. The dark gray color represents the least square means for the effect of line, and light gray represents the least square means for the effect of time.

corresponding to the increased number of cells neighboring the giant feeding cells. The observed increased proportion of nuclei > 16C in galls, compared with uninfected roots, reveals that these high ploidy levels probably derive from nuclei isolated from GCs induced by RKNs. Galls in roots of the $KRP1^{OE}$ line contained a higher percentage of cells with a DNA content above 4C, a two-fold increase in those with a DNA content of 8C and additional nuclei with 16C, 32C and 64C (Fig. 8c). In contrast, $KRP2^{OE}$ galls showed increased 2C levels, and a two-fold decrease in nuclei with higher ploidy levels (4C to 64C) compared with wild type or the $KRP1^{OE}$ line (Fig. 8d).

KRP2 protein levels are regulated during NFS development

In order to determine the subcellular localization of KRP2 in uninfected and nematode-infected plant cells, we generated *35S:GFP-KRP2* constructs, which were firstly expressed in BY2 cells. Protein localization was then tracked by time-lapse confocal microscopy in BY2 cells (Movie S4). Secondly, we also recorded protein localization in roots of transgenic Arabidopsis plants (Fig. 9), and, taken together, our data show that KRP2 was localized in the nucleus during interphase and early pre-prophase (Fig. 9; Movie S4). After nuclear envelope breakdown at late prophase, GFP fluorescence of KRP2 was dispersed into the cytoplasm. Throughout mitosis, a remaining weak fluorescence of KRP2 was seen within the cytoplasm. During cytokinesis, a progressive accumulation of KRP2 was observed in the nuclei of the daughter cells (Fig. 9; Movie S4).

The localization and dynamics of GFP-KRP2 in galls showed that protein levels were variable in the nuclei of GCs, while strong fluorescence was recorded in neighboring cells (Fig. 10). During the mitotic activity phase (7 and 14 DAI), GFP-KRP2 fluorescence in GC nuclei was weak and was visibly associated with the presence of the nematode (Fig. 10a,b; Movie S5). At later developmental stages (21–40 DAI), when mitotic activity ceased in GCs, and expansion of nuclei and GCs took place (Fig. 10c), GFP-KRP2 fluorescence became brighter. In contrast, GFP fluorescence in $KRP1^{OE}$ in GCs and neighboring cell nuclei was strong and stable throughout all stages of nematode infection (Fig. S11a). Fluorescence intensities in plants expressing only free GFP were used as a control and were found to be stable throughout gall development (Fig. S11b).

Ectopic expression of *KRP* blocks nematode development and severely reduces the number of offspring

Morphological analyses showed that the ectopic expression of the *KRP1* and *KRP2* genes disturbed gall ontogeny. In both lines, infective J2 nematodes were able to penetrate and migrate along the roots, and induce galls. However, at 40 DAI, both the $KRP1^{OE}$ and $KRP2^{OE}$ lines showed a 75–80% reduction in gall number and gall size (Fig. 11a–c), followed by a significant reduction in egg mass number compared with infected wild-type roots (Fig. 11a,b). Infected roots (at 40 DAI) were stained with acid fuchsin to identify the developmental stage of the nematodes. Whereas in wild-type plants, most of the pear-shaped females reached reproductive maturity at late stages of nematode infection (40 DAI), in both the $KRP1^{OE}$ and $KRP2^{OE}$ lines most nematodes remained as second-stage juveniles and were associated with reduced feeding sites within plant roots (Fig. 11c).

Discussion

The *KRP* gene family is active in the cell cycle machinery of nematode feeding sites

Herein we report the major involvement of cell cycle inhibitor genes in the control of NFS development. The present work focused on an investigation of the *KRP* gene family during gall development induced by *M. incognita* in Arabidopsis roots. Using *KRP* promoter-GUS fusions and mRNA *in situ* hybridization, we showed that *KRP2*, *KRP5* and *KRP6* are expressed in galls after nematode infection. In contrast, the remaining Arabidopsis *KRP* genes (*KRP1*, *KRP3*, *KRP4* and *KRP7*) did not show any transcriptional activity in galls. Consistent with this finding, almost no expression of the same genes was seen in the vascular tissue at the root elongation zone of uninfected roots, a region that

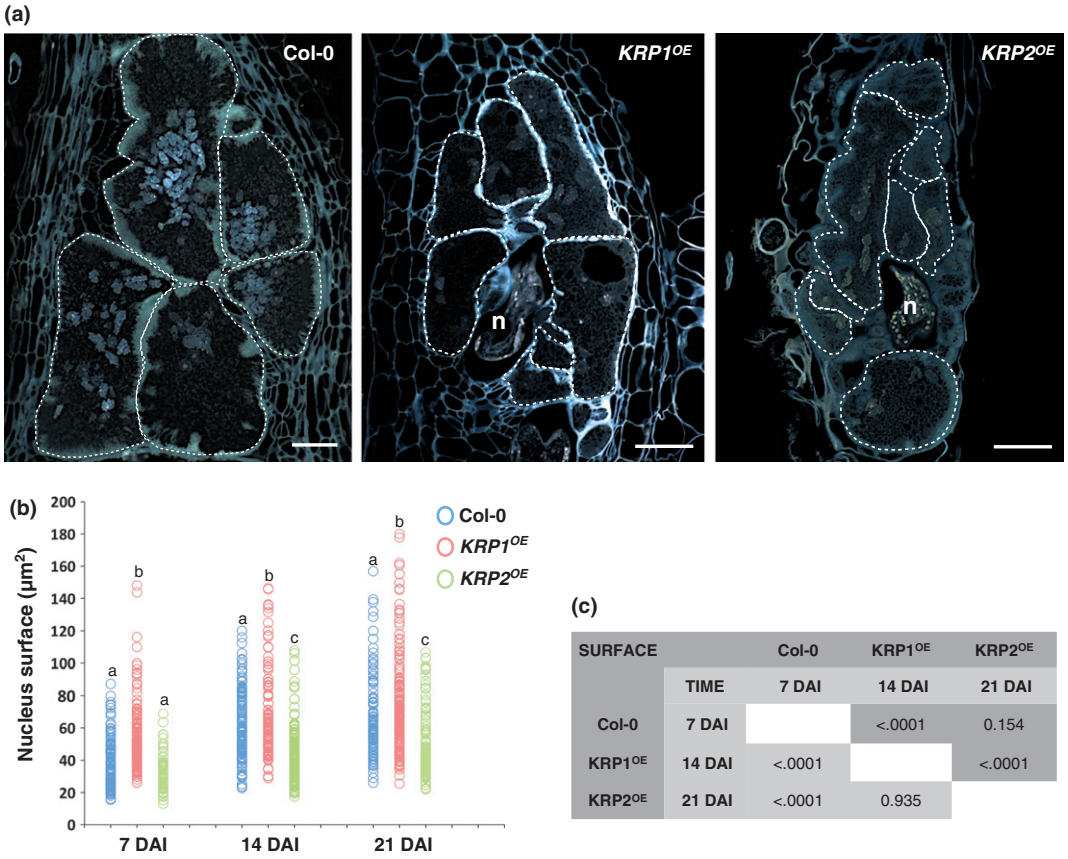

(c)

SURFACE		Col-0	KRP1^{OE}	KRP2^{OE}
	TIME	7 DAI	14 DAI	21 DAI
Col-0	7 DAI		<.0001	0.154
KRP1^{OE}	14 DAI	<.0001		<.0001
KRP2^{OE}	21 DAI	<.0001	0.935	

Fig. 6 Cell cycle inhibition caused by Kip-related protein (KRP) overexpression affects nuclear division and size. (a) 4,6-Diamidino-2-phenylindole (DAPI) staining of wild-type gall tissues compared with *KRP1*^{OE} and *KRP2*^{OE} overexpressing lines at 40 d after inoculation (DAI). White circles delimit giant cells. Bars, 50 µm. (b) Measurements (µm^2) of giant cell nuclei (minimum of 80) in the wild type and *KRP* overexpressing lines at different stages of nematode infection (7, 14 and 21 DAI). Different letters indicate statistically significant differences among KRPs at each time-point after nematode infection ($P < 0.0001$). (c) Multiple overall comparisons of nucleus surface expansion. The dark gray color represents the least square means for the effect of line, and the light gray color represents the least square means for the effect of time.

nematodes normally infect. These data suggest that nematodes manipulate the existing cell cycle machinery of the root host in their favor, by inducing the same *KRP* genes as are expressed in the root vascular tissues. Differences in GUS activity among the seven *KRP* genes at various stages of the development of NFSs suggest diverse roles of these genes during this plant–RKN interaction. In particular, *KRP2* and *KRP5* promoter activities were high during the later stages of GC development (14–21 DAI), compared, for example, with the decreased expression of *KRP6* at similar stages. Up-regulation of *KRP2* during RKN infection has also been reported in transcriptomic analysis, confirming the involvement of this cell cycle inhibitor during gall development (Jammes *et al.*, 2005).

Promoter activity provided useful information on transcription of these genes in feeding sites, while *in vivo* observations, particularly of KRP2, suggested the post-translational regulation of KRPs during nematode infection. KRP2 localization during mitosis is reported here for the first time in BY2 cells, and *in planta*, for noninfected and nematode-infected Arabidopsis root cells. During the phase of high mitotic activity in GCs (7–14 DAI), low GFP-KRP2 fluorescence was observed within the GCs, associated with the presence of the feeding nematode. Fluctuation of KRP2 protein levels in GCs suggests a controlled molecular dialogue between the plant host and the nematode, and that protein levels must be below a certain threshold to allow the progression of the mitotic activity within the GCs. This is likely to occur via nematode secretions that might directly interact with the KRPs of the plant host or via the induction of changes in host gene expression.

The KRP2 protein is negatively regulated at the post-translational level by B-type CDKs (Verkest *et al.*, 2005a), and it has been shown that the *CDKB1;1* promoter is strongly active in young galls (de Almeida Engler *et al.*, 1999). Accordingly, when decreased *CDKB1;1* expression was observed in galls at intermediate to late developmental stages (14–21 DAI), increasing KRP2 protein levels were observed in GCs *in vivo*. When there is less mitotic activity in GCs, KRP2 accumulation in their nuclei may regulate the levels of the mitotic CDK/CYC complex, which is associated with the switch to the endocycle. At this stage, nuclei enlarge in GCs, suggesting that inhibition of CDKA activity allows progression through the endocycle.

KRP loss of function induces mitosis in galls

Assessment of *KRP* loss-of-function mutants (*krp2*, *krp2*$^{-/-}$ *krp6*$^{-/-}$ and *krp*∂) showed an increased number of nuclei in GCs

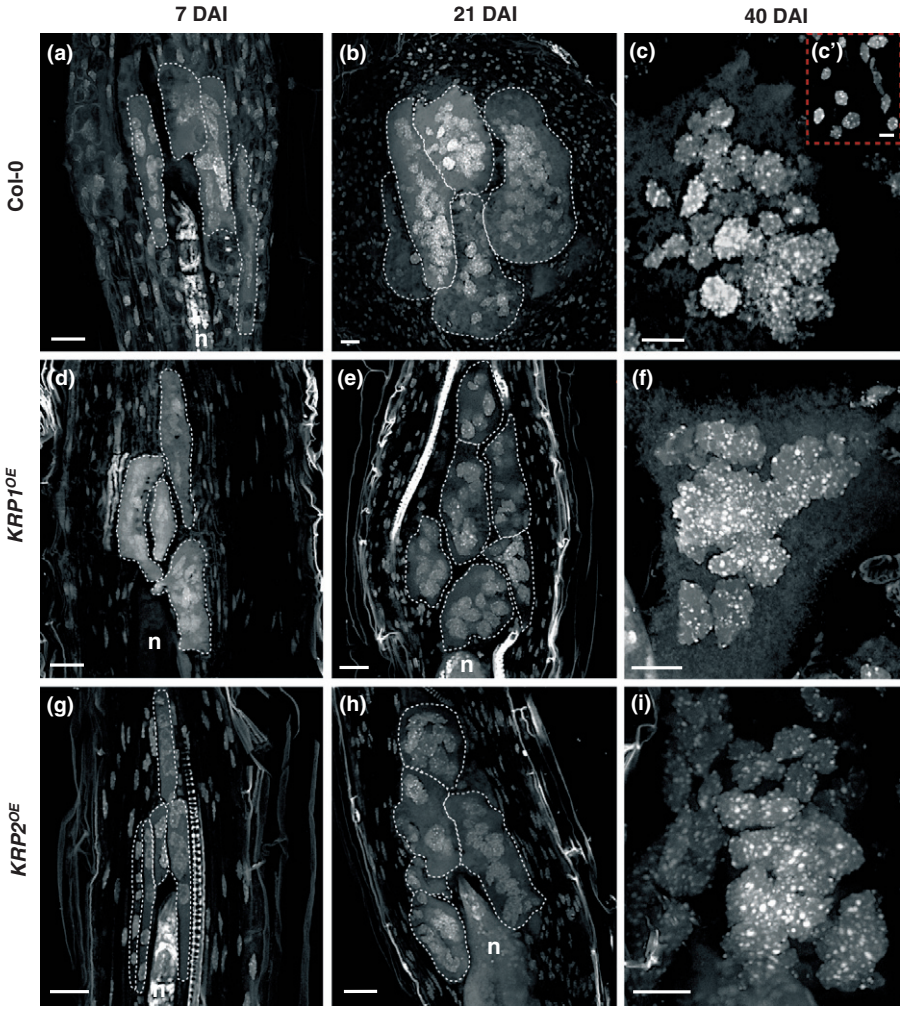

Fig. 7 Giant cells of *Meloidogyne incognita*-induced Arabidopsis galls in the *KRP1*^{OE} and *KRP2*^{OE} lines contain fewer nuclei than in the wild type. 3D confocal projections of serial optical sections of whole-mount root samples cleared and stained with propidium iodide (PI) are shown. White circles delimit giant cells. (a, b) Wild-type galls at 7 and 21 d after inoculation (DAI). (d, e) *KRP1*^{OE} galls at 7 and 21 DAI. Fewer but larger nuclei are observed in giant cells. (g, h) *KRP2*^{OE} galls at 7 and 21 DAI. Fewer nuclei are observed in giant cells. (c, c′, f, i) Detailed images of nuclei in uninfected wild-type roots (c′), wild-type galls 40 DAI (c), *KRP1*^{OE} galls 40 DAI (f), and *KRP2*^{OE} galls 40 DAI (i). Note bright PI-stained spots in nuclei with variable intensities, indicative of chromocentric regions and/or heterochromatin foci. Bars, 20 μm; (c′) 5 μm.

and proliferation of neighboring cells, when compared with wild-type galls. These observations suggest an intense mitotic activity in *krp* mutants compared with the wild type. Loss of function in the *krp2* line of Arabidopsis may result in increased levels of CYCD/CDKA activity, enhancing the potential for cell division, demonstrated by the increased number of lateral roots in the same mutants (Sanz *et al.*, 2011). Our previous data demonstrated the up-regulation of cyclins in GCs upon RKN infection (de Almeida Engler *et al.*, 1999, 2011). Hence, the probable accumulation of CDKA;1 in gall tissues in the loss-of-function mutants may superactivate the CDK/CYC complexes in the absence of KRPs (Boruc *et al.*, 2010b), which would cause cells to enter the mitotic phase more rapidly during gall development. The end result is the abnormal increase in the number of nuclei observed in GCs, and the intense proliferation of neighboring cells. Excessive amounts of CDKA/CYC complexes in GCs could extend their mitotic phase for a longer period, resulting in a delayed switch to the endocycle phase (de Almeida Engler & Gheysen, 2013). Nevertheless, no significant effect on nematode development, or reproduction, was observed in any of the loss-of-function mutants. A larger number of nuclei in GCs may compensate for the decreased nuclear amplification, resulting in normal egg laying.

Ectopic *KRP* expression drastically impairs gall and nematode development and induces variation in ploidy levels in feeding sites

The inhibitory effect of *KRP* genes on cell cycle progression in galls was examined by using strong *KRP1* and *KRP2* overexpressing lines. All members of the Arabidopsis *KRP* family have primarily affinity for CDKA;1, which is considered the *bona fide* plant CDK, required for both G1/S and G2/S transitions (Van Leene *et al.*, 2010b; De Veylder *et al.*, 2011). It has been shown that the two KRPs (KRP1 and KRP2) studied here directly bind to both CDKA;1 and D-type cyclins, and their respective complexes (De Veylder *et al.*, 2001; Verkest *et al.*, 2005a; Boruc *et al.*, 2010b; Van Leene *et al.*, 2010b). Although the order of events occurring during the cell cycle in GCs is not fully understood, mitotic events should mainly take place during the first 2 wk after NFS induction (up to 14 DAI); after mitotic events cease, there seems to be a period of DNA amplification related to the endoreduplication cycle (de Almeida Engler & Gheysen, 2013). Thus, ectopic expression of *KRP1* and *KRP2* in young galls possibly triggers the inactivation of mitotic CDKs, resulting in the inhibition of mitosis. Consequently, nuclear division is reduced in GCs and a severe decline in neighboring cell division is observed,

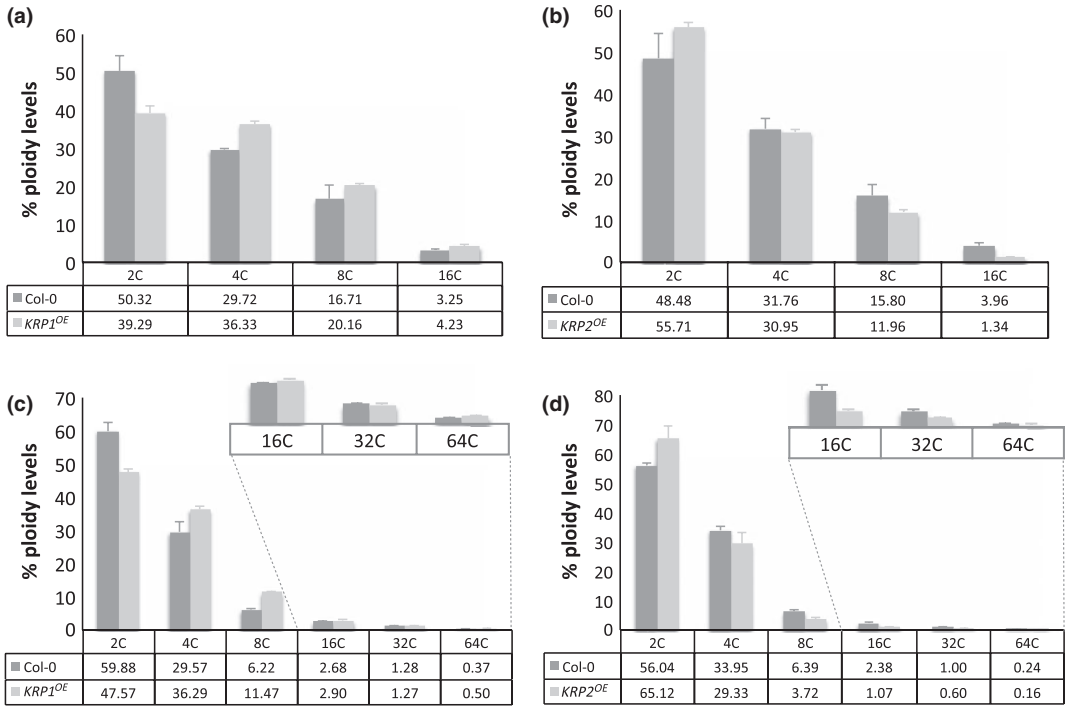

Fig. 8 Ploidy levels of galls are differently affected in *KRP1*^{OE} and *KRP2*^{OE} lines compared with the wild type. (a, b) Percentage of nuclei with various ploidy levels in gall-less wild-type root segments compared with *KRP1*^{OE} (a) and *KRP2*^{OE} (b). (c, d) Percentage of ploidy levels in galls (40 d after inoculation (DAI)). In *KRP1*^{OE}, a noteworthy increase in nuclei with high ploidy levels was observed (c). Conversely, in the *KRP2*^{OE} line, galls displayed a significant reduction in nuclei with high ploidy levels (> 16C) compared with nuclei of wild-type galls (d). Error bars represent standard deviation.

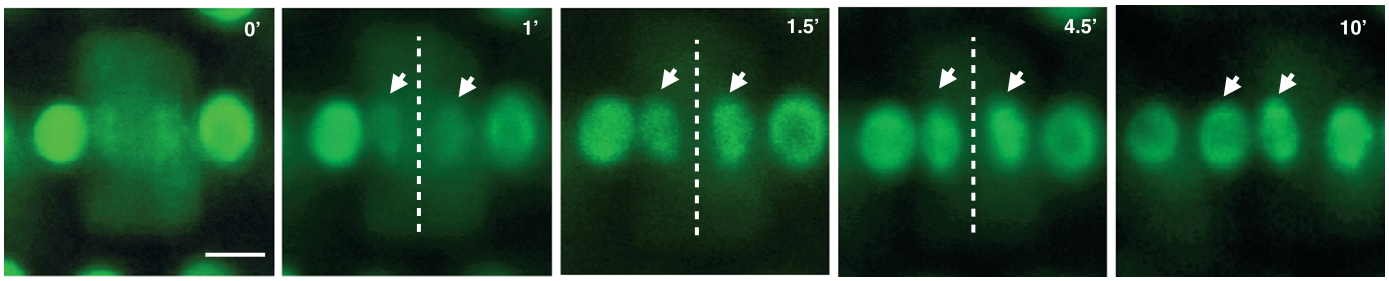

Fig. 9 Nuclear localization of GFP-KRP2 in interphase Arabidopsis root cells disappears during mitosis. Images taken over a time lapse of 10 min show mitotic cell division in Arabidopsis root cells. Dashed white lines indicate the separation plane of two new daughter cells formed after cell division. Arrows indicate the nucleus of each new daughter cell. The time is indicated in the top right corner of each confocal image. Bar, 5 μm.

causing a drastic reduction in gall size. Previous work has demonstrated the presence of plasmodesmata between GCs and neighboring cells, suggesting their connection with GC development (Hofman *et al.*, 2010), and their involvement in nutrient transfer to the giant feeding cells (Hoth *et al.*, 2008). Therefore, the reduced numbers of neighboring cells observed in galls overexpressing *KRP1* and *KRP2* might have an impact on nutrient supply to GCs.

The enlargement of nuclei often occurring in plant cells is probably linked to endoreduplication and/or endomitosis (Sugimoto-Shirasu & Roberts, 2003; De Veylder *et al.*, 2011). An increased DNA content of GC nuclei, from 6.5 to 15.8 times that of uninfected root tip cells, has been observed by Feulgen microspectrophotometry in lettuce (*Lactuca sativa*) and pea (*Pisum sativum*) galls, respectively (Wiggers *et al.*, 1990). Similarly, nodules formed during the *Sinorhizobium–Medicago* symbiosis show a nuclear DNA content increase up to 64C and root cells are drastically enlarged (Kondorosi & Kondorosi, 2004). Cleared and PI-stained whole GCs show that densely stained foci in interphase nuclei correspond to heterochromatic regions. In the present study, GC nuclei contained > 20 intensely and differentially stained heterochromatin foci compared with the typical 10 chromocenters of reduced size observed in uninfected interphase root cells. Chromocenters are densely packed heterochromatic regions corresponding to centromeres and nuclear organizing regions (Fransz *et al.*, 2002). The increased size and number of these chromocenter-like spots is indicative of polyploidization occurring in Arabidopsis (Maluszynska & Heslop-Harrison, 1993; Kato & Lam, 2003; Berr & Schubert, 2007). The variable size and number of heterochromatin nuclear

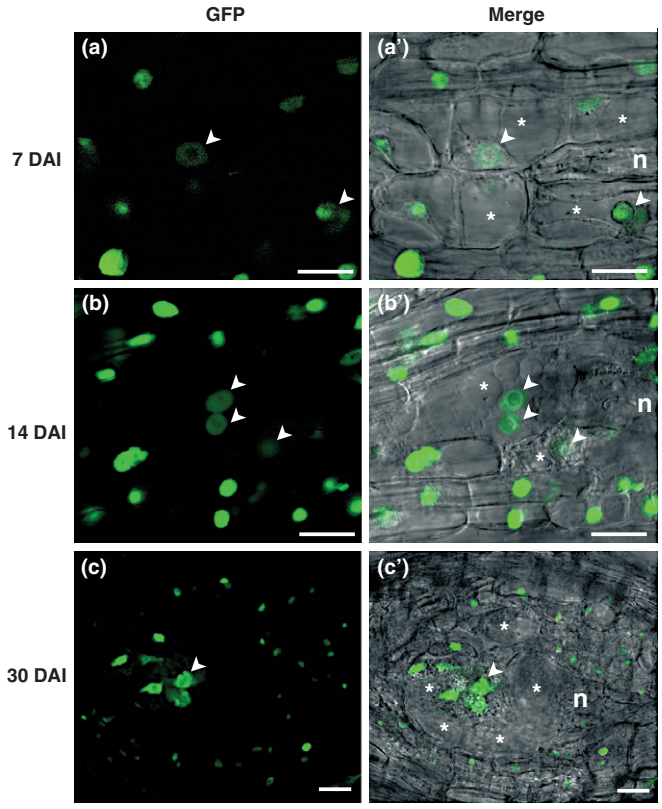

Fig. 10 Kip-related protein 2 (KRP2) protein levels in giant cells appear to be regulated during nematode parasitism. (a–c) *In vivo* localization of GFP-KRP2 (green) in the gall nuclei. GFP-KRP2 localization in giant cell nuclei (arrow) at 7 d after inoculation (DAI) (a, a'), 14 DAI (b, b') and 30 DAI (c, c') is shown. Bars, 20 μm.

foci in GC nuclei might result from the rearranged heterochromatin architecture. These interphase nuclear heterochromatin foci are typically associated with high ploidy levels (Schubert *et al.*, 2006; Berr & Schubert, 2007), and could be correlated with an increase of transcriptional activity occurring in GCs (Jammes *et al.*, 2005; Damiani *et al.*, 2012).

The importance of polyploidization for gall maturation has been demonstrated recently by the observation that GC nucleus size and expansion are dramatically affected in plants with impaired endocycle machinery (de Almeida Engler *et al.*, 2012). While nuclei of Arabidopsis root cells may undergo up to four rounds of endoreduplication, reaching a maximum of 16C, flow cytometry analyses of wild-type galls revealed nuclei with up to 64C. The heterogeneity within the higher ploidy levels (8C to 64C) reflects the nuclei of variable sizes observed in GCs. The low (2C to 4C) ploidy levels derive from cells neighboring the giant feeding cells, which continuously divide during gall formation. Studies have shown that the expression levels of KRPs have an intimate relationship with the onset of endoreduplication in Arabidopsis in a dosage-dependent manner (Verkest *et al.*, 2005a; Roeder *et al.*, 2010). In the *KRP1*^{OE} line, the two-fold increase in nuclei number displaying higher ploidy levels in galls suggests a faster shift from mitosis to the endocycle, although the accelerated early entry into the endocycle in the *KRP1*^{OE} line inhibited GC expansion. Conversely, high *KRP2* levels resulted in few and small nuclei with reduced ploidy levels. GCs displayed a reduction in the number of endoreduplicating nuclei (decreased 32C and 64C levels). Nevertheless, even when *KRP2* overexpression in galls inhibited both mitosis and the endocycle, the feeding nematode remained capable of ectopically inducing DNA replication to a certain extent, suggesting a resilient RKN control of the cell cycle during the infection of root cells. Hence, nematode-secreted proteins could play a role in redirecting cell cycle regulation via modulation of proteins such as KRPs to ensure NFS development.

Here we have identified for the first time a cell cycle gene that has a major negative effect on gall size and consequently strongly influences nematode reproduction. Ectopic expression of KRP4 has less effect on nematode reproduction even when nuclei presented altered morphology (Vieira *et al.*, 2012). Therefore, morphological observations and infection tests suggest that different members of the KRP family have distinct functions in feeding cell development. The drastic reduction in root-knot or gall size observed in the *KRP1*^{OE} and *KRP2*^{OE} lines was shown to be caused by substantial reductions in GC size and in mitotic activity in neighboring cells. Consequently, this resulted in a marked decrease in nematode body size, which depends on an abundant food supply from the host cells. This high metabolic demand for energy and carbon for the feeding nematodes and the effective function of GCs as transfer cells and a food source for RKNs have been long recognized (Jones & Northcote, 1972; Baldacci-Cresp *et al.*, 2012). As such, feeding sites are indispensable for nematode survival and development, and the *bona fide* inhibition of cell cycle CDK/CYC complexes through overexpression of *KRP1* and *KRP2* shown here compromised the nematode's life cycle, leading to a reduction in the number of nematode offspring.

Concluding remarks

We report here that by overexpressing the cell cycle inhibitors *KRP1* and *KRP2* the typical root-knot or gall structures are arrested early in development in the host root. KRP2, which is naturally expressed in galls, may be important for adjusting CDK activity in feeding sites to drive and control the transition between different cell cycle programs, such as the mitotic activity or entering endoreduplication cycles (Inzé & De Veylder, 2006; De Veylder *et al.*, 2011). However, ectopic expression of certain KRPs during gall development may lead to the inactivation of CDKA/CYCD complexes, impairing progression of both cell cycle mechanisms and consequently interfering with the fate and maintenance of GCs. CDK inhibitors have been used as an effective strategy for cancer control in humans to specifically arrest the cell cycle in tumor cells (Malumbres *et al.*, 2007; Benson *et al.*, 2008). Similarly, engineering ectopic expression of genes such as *KRP1* and *KRP2*, using promoters preferentially active in galls, might be a valuable strategy to control root-knot growth. An analogous strategy might be envisaged to control the infection of other plant pathogens that exploit the host cell cycle machinery.

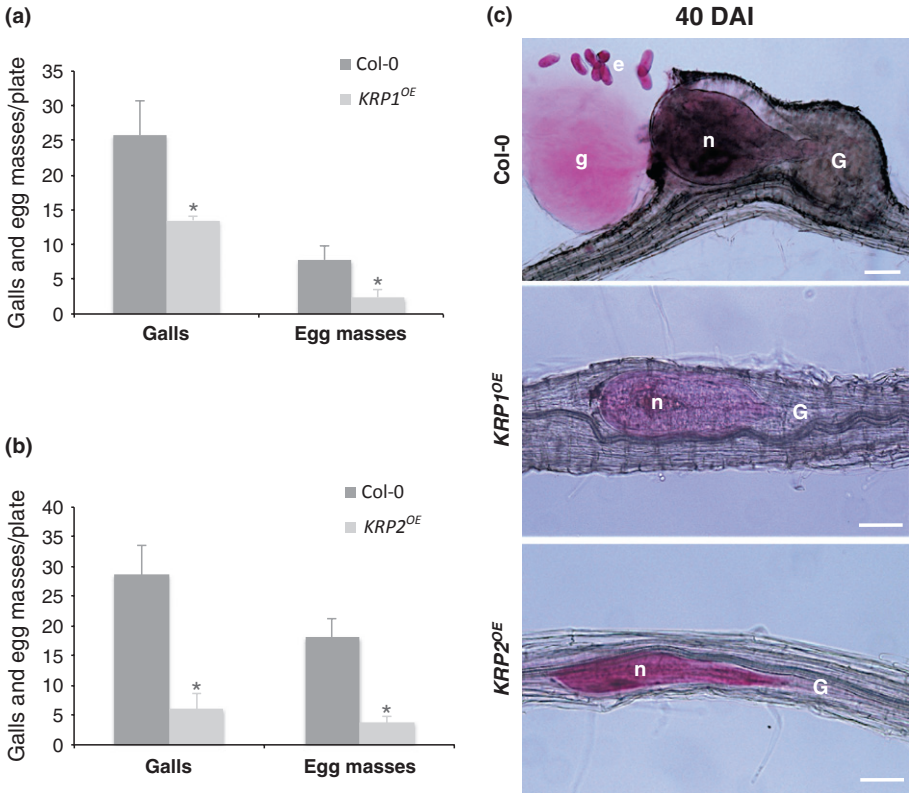

Fig. 11 Ectopic expression of Kip-related protein 1 (*KRP1*) and *KRP2* drastically impairs gall, egg mass and nematode development. (a, b) Nematode infection tests of *KRP* overexpression lines compared with the wild type. Data shown represent means ± SD from two independent biological repetitions, in which a minimum of 60 seedlings of each line were evaluated for the nematode infection test. Pairwise comparisons were made using Student's *t*-test ($P \leq 0.05$). (c) Acid fuchsin staining of galls 40 d after inoculation (DAI). Galls in $KRP1^{OE}$ and $KRP2^{OE}$ lines were drastically reduced compared with the wild type. In most galls, the females did not reach maturity and consequently did not produce eggs. e, eggs; G, gall; g, gelatinous matrix; n, nematode. Bars, 50 μm.

Acknowledgements

We thank E. Wajnberg for help with the statistical analyses in Figs 5 and 6, F. Diaz, M. Y. Serrano, I. M. Torres, L. Merino and A. C. Bombin for help with analyses of *KRP* lines, S. Pagnotta for the electron microscopy, and G. De Jaeger for fruitful discussions. We also thank C. Luschnig for providing the *krp0* line. P.V. has been supported by a doctoral scholarship from Fundação para a Ciência e Tecnologia, Portugal (SFHR\BD \41339\2007).

References

de Almeida Engler J, De Veylder L, De Groodt R, Rombauts S, Boudolf V, De Meyer B, Hemerly A, Ferreira P, Beeckman T, Karimi M *et al.* 2009. Molecular markers and cell cycle inhibitors show the importance of cell cycle progression in nematode-induced galls and syncytia. *Plant Journal* **59**: 645–660.

de Almeida Engler J, De Vleesschauwer V, Burssens S, Celenza JLJ, Inzé D, Van Montagu M, Engler G, Gheysen G. 1999. Molecular markers and cell cycle inhibitors show the importance of cell cycle progression in nematode-induced galls and syncytia. *The Plant Cell* **11**: 793–808.

de Almeida Engler J, Engler G, Gheysen G. 2011. Unravelling the plant cell cycle in nematode induced feeding sites. In: Jones J, Gheysen G, Fenoll C, eds. *Genomics and molecular genetics of plant–nematode interactions*. Dordrecht, the Netherlands: Springer Science+Business Media, 349–368.

de Almeida Engler J, Gheysen G. 2013. Nematode-induced endoreduplication in plant host cells: why and how? *Molecular Plant-Microbe Interactions* **26**: 17–24.

de Almeida Engler J, Kyndt T, Vieira P, Van Cappelle E, Bouldolf V, Sanchez V, Escobar C, De Veylder L, Engler G, Abad P *et al.* 2012. *CCS52* and *DEL1* genes are key components of the endocycle in nematode induced feeding sites. *Plant Journal* **72**: 185–198.

Anzola JM, Sieberer T, Ortbauer M, Butt H, Korbei B, Weinhofer I, Mullner AE, Luschnig C. 2010. Putative *Arabidopsis* transcriptional adaptor protein (PROPORZ1) is required to modulate histone acetylation in response to auxin. *Proceedings of the National Academy of Sciences, USA* **107**: 10308–10313.

Baldacci-Cresp F, Chang C, Maucourt M, Deborde C, Hopkins J, Lecomte P, Bernillon S, Broquisse R, Moing A, Abad P *et al.* 2012. (Homo)glutathione deficiency impairs root-knot nematode development in *Medicago truncatula*. *Plos Pathogens* **8**: e1002471.

Barrôco RM, Peres A, Droual AM, De Veylder L, Nguyen LSL, De Wolf J, Mironon V, Peerbolte R, Beemster GTS, Inzé D *et al.* 2006. The cyclin-dependent kinase inhibitor Orysa KRP1 plays an important role in seed development of *Oryza sativa*. *Plant Physiology* **142**: 1053–1064.

Beeckman T, Engler G. 1994. An easy technique for the clearing of histochemically stained plant tissue. *Plant Molecular Biology Reporter* **12**: 37–42.

Bemis SM, Torii KU. 2007. Autonomy of cell proliferation and developmental programs during *Arabidopsis* aboveground organ morphogenesis. *Developmental Biology* **304**: 367–381.

Benson A, Dowdy SF, Roberts JM. 2008. CDK inhibitors: cell cycle regulators and beyond. *Developmental Cell* **14**: 159–169.

Berr A, Schubert I. 2007. Interphase chromosome arrangement in *Arabidopsis thaliana* is similar in differentiated and meristematic tissues and shows a transient mirror symmetry after nuclear division. *Genetics* **176**: 853–863.

Bird DA, Buruiana MM, Zhou Y, Fowke LC, Wang H. 2007. *Arabidopsis* cyclin-dependent kinase inhibitors are nuclear-localized and show different localization patterns within the nucleoplasm. *Plant Cell Reports* **26**: 861–872.

Bisbis B, Delmas F, Joubes J, Sicard A, Hernould M, Inzé D, Mouras A, Chevalier C. 2006. Cyclin-dependent kinase inhibitors regulate the CDK/cyclin complex activities in endoreduplicating cells of developing tomato fruit. *The Journal of Biological Chemistry* **281**: 7374–7383.

Boruc J, Mylle E, Duda M, De Clercq R, Rombauts S, Geelen D, Hilson P, Inzé D, Van Damme D, Russinova E. 2010a. Systematic localization of the *Arabidopsis* core cell cycle proteins reveals novel cell division complexes. *Plant Physiology* **152**: 553–565.

Boruc J, Van den Daele H, Hollunder J, Rombauts S, Mylle E, Hilson P, Inzé D, De Veylder L, Russinova E. 2010b. Functional modules in the Arabidopsis core cell cycle binary protein-protein interaction network. *Plant Cell* **22**: 1264–1280.

Caillaud M-C, Dubreuil G, Quentin M, Perfus-Barbeoch L, Lecomte P, de Almeida Engler J, Abad P, Rosso MN, Favery B. 2008. Root-knot nematodes manipulate plant cell functions during a compatible interaction. *Journal of Plant Physiology* **165**: 104–113.

Churchman ML, Brown ML, Kato N, Kirik V, Hülskamp M, Inzé D, De Veylder L, Walker JD, Zheng Z, Oppenheimer DG *et al.* 2006. SIAMESE, a novel plant-specific cell cycle regulator controls endoreplication onset in *Arabidopsis thaliana*. *The Plant Cell* **18**: 3145–3157.

Coelho CM, Dande RA, Sabelli PA, Sun Y, Dilkes BP, Gordon-Kamm WJ, Larkins BA. 2005. Cyclin-dependent kinase inhibitors in maize endosperm and their potential role in endoreduplication. *Plant Physiology* **138**: 2323–2336.

Comai L. 2005. The advantages and disavantages of being polyploid. *Nature Reviews Genetics* **6**: 836–846.

Damiani I, Baldacci-Cresp F, Hopkins J, Andrio E, Balzergue S, Lecomte P, Puppo A, Abad P, Favery B, Hérouart D. 2012. Plant genes involved in harbouring symbiotic rhizobia or pathogenic nematodes. *New Phytologist* **194**: 511–522.

De Veylder L, Beeckman T, Beemster GT, Krois L, Terras F, Landrieu I, Van der Schueren E, Maes S, Naudts M, Inzé D. 2001. Functional analysis of cyclin-dependent kinase inhibitors of *Arabidopsis*. *The Plant Cell* **13**: 1653–1667.

De Veylder L, Larkin JC, Schnittger A. 2011. Molecular control and function of endoreduplication in development and physiology. *Trends in Plant Science* **16**: 1360–1385.

Edgar BA, Orr-Weaver TL. 2001. Endoreplication cell cycles: more for less. *Cell* **105**: 297–306.

Fransz P, De Jong JH, Lysak M, Ruffini Castiglione M, Schubert I. 2002. Interphase chromosomes in *Arabidopsis* are organised as well-defined chromocenters from which euchromatin loops emanate. *Proceedings of the National Academy of Sciences, USA* **99**: 14584–14589.

Galbraith DW, Harkins KR, Knapp S. 1991. Systemic endopolyploidy in *Arabidopsis thaliana*. *Plant Physiology* **96**: 985–989.

Geelen DNV, Inzé DG. 2001. A bright future for the Bright Yellow-2 cell culture. *Plant Physiology* **127**: 1375–1379.

Gheysen G, Fenoll C. 2002. Gene expression in nematode feeding sites. *Annual Review of Phytopathology* **40**: 191–219.

Hofman J, Youssef-Banora M, de Almeida Engler J, Grundler FM. 2010. The role of callose deposition along plasmodesmata in nematode feeding sites. *Molecular Plant-Microbe Interactions* **23**: 549–557.

Hoth S, Stadler R, Sauer N, Hammes UZ. 2008. Differential vascularization of nematode-induced feeding sites. *Proceedings of the National Academy of Sciences, USA* **105**: 12617–12622.

Inzé D, De Veylder L. 2006. Cell cycle regulation in plant development. *Annual Review of Genetics* **40**: 77–105.

Jammes F, Lecomte P, de Almeida Engler J, Bitton F, Martin-Magniette ML, Renou JP, Abad P, Favery B. 2005. Genome-wide expression profiling of the host response to root-knot nematode infection in *Arabidopsis*. *Plant Journal* **44**: 447–458.

Jasinski S, Perennes C, Bergounioux C, Glab N. 2002. Comparative molecular and functional analyses of the tobacco cyclin-dependent kinase inhibitor NtKIS1a and its spliced variant NtKIS1b. *Plant Physiology* **130**: 1871–1882.

Jones MGK, Northcote DH. 1972. Multinucleate transfer cells induced in coleus roots by the root-knot nematode, *Meloidogyne arenaria*. *Protoplasma* **75**: 381–395.

Joubès J, Chevalier C. 2000. Endoreduplication in higher plants. *Plant Molecular Biology* **43**: 735–745.

Kang J, Mizukami Y, Wang H, Fowke L, Dengler NG. 2007. Modification of cell proliferation patterns alters leaf vein architecture in *Arabidopsis thaliana*. *Planta* **226**: 1207–1218.

Karimi M, Inzé D, Depicker A. 2002. GATEWAY™ vectors for *Agrobacterium*-mediated plant transformation. *Trends in Plant Science* **7**: 193–195.

Kato N, Lam EJ. 2003. Chromatin of endoreduplicated pavement cells has greater range of movement than that of diploid guard cells in *Arabidopsis thaliana*. *Journal of Cell Science* **116**: 2195–2201.

Kondorosi E, Kondorosi A. 2004. Endoreduplication and activation of the anaphase-promoting complex during symbiotic cell development. *FEBS Letters* **567**: 152–157.

Malumbres M, Pevarello P, Barbacid M, Bischoff JR. 2007. CDK inhibitors in cancer therapy: what is next? *Trends in Pharmacological Sciences* **29**: 16–21.

Maluszynska J, Heslop-Harrison JS. 1993. Molecular cytogenetics of the genus *Arabidopsis*: in situ localization of rDNA sites, chromosome numbers and diversity in centromeric heterochromatin. *Annals of Botany* **71**: 479–484.

Niebel A, de Almeida Engler J, Hemerly A, Ferreira P, Van Montagu M, Gheysen G. 1996. Induction of *cdc2a* and *cyc1At* expression in *Arabidopsis* during early phases of nematode-induced feeding cell formation. *Plant Journal* **10**: 1037–1043.

Ormenese S, de Almeida Engler J, de Groot R, de Veylder L, Inzé D, Jacqmard A. 2004. Analysis of the spatial expression pattern of seven Kip related proteins (KRPs) in the shoot apex of *Arabidopsis thaliana*. *Annals of Botany* **93**: 575–580.

Peres A, Churchman ML, Hariharan S, Himanen K, Verkest A, Vandepoele K, Magyar Z, Hatzfeld Y, Van Der Schueren E, Beemster GT *et al.* 2007. Novel plant-specific cyclin-dependent kinase inhibitors induced by biotic and abiotic stresses. *The Journal of Biological Chemistry* **282**: 25588–25596.

Pettko-Szandtner A, Meszaros T, Horvath GV, Bakó L, Csordás-Tóth E, Blastyák A, Zhiponova M, Miskotczi P, Dudits P. 2006. Activation of an alfalfa cyclin-dependent kinase inhibitor by calmodulin-like domain protein kinase. *Plant Journal* **46**: 111–123.

Roeder AHK, Chickarmane V, Cunha A, Obara B, Manjunath BS, Meyerowitz EM. 2010. Variability in the control of cell division underlies sepal epidermal patterning in *Arabidopsis thaliana*. *PLoS Biology*: **8** e1000367.

Sanz L, Dewitte W, Forzani C, Patell F, Nieuwland J, Wen B, Quelhas P, De Jager S, Titmus C, Campilho A *et al.* 2011. The *Arabidopsis* D-type cyclin CYCD2;1 and the inhibitor ICK2/KRP2 modulate auxin-induced lateral root formation. *The Plant Cell* **23**: 1–20.

Schubert V, Klatte M, Pecinka A, Meister A, Jasencakova Z, Schubert I. 2006. Sister chromatids are often incompletely aligned in meristematic and endopolyploid interphase nuclei of *Arabidopsis thaliana*. *Genetics* **172**: 467–475.

Sugimoto-Shirasu K, Roberts K. 2003. "Bit it up": endoreduplication and cell-size control in plants. *Current Opinion in Plant Biology* **6**: 544–553.

Van de Capelle E, Plovie E, Kyndt T, Grunewald W, Cannoot B, Gheysen G. 2008. *AtCDK;1* silencing in *Arabidopsis thaliana* reduces reproduction of sedentary plant-parasitic nematodes. *Plant Biotechnology Journal* **6**: 749–757.

Van Leene J, Boruc J, De Jaeger G, Russinova E, De Veylder L. 2010b. A Kaleidoscopic view of the *Arabidopsis* core cell cycle interactome. *Trends in Plant Science* **16**: 141–150.

Van Leene J, Hollunder J, Eeckhout D, Persiau G, Van De Slijke E, Stals H, Van Isterdael G, Verkest A, Neirynck S, Buffel Y *et al.* 2010a. Targeted interactomics reveals a complex core cell cycle machinery in *Arabidopsis thaliana*. *Molecular Systems Biology* **6**: 397.

Verkest A, de O Manes C-L, Vercruysse M, Maes S, Van Der Schueren E, Beeckman T, Genschik P, Kuiper M, Inzé D, De Veylder L. 2005b. The cyclin-dependent kinase inhibitor KRP2 controls the mitosis-to-endocycle transition during *Arabidopsis* leaf development through a specific inhibition of the mitotic CDKA;1 kinase complexes. *The Plant Cell* **17**: 1723–1736.

Verkest A, Weinl C, Inzé D, De Veylder L, Schnittger A. 2005a. Switching the cell cycle. Kip-Related Proteins in plant cell cycle control. *Plant Physiology* **139**: 1099–1106.

Vieira P, Engler G, de Almeida Engler J. 2012. Whole-mount confocal imaging of nuclei in giant feeding-cells induced by root-knot nematodes in *Arabidopsis*. *New Phytologist* **195**: 488–496.

Wang H, Fowke LC, Crosby WL. 1997. A plant cyclin-dependent kinase inhibitor gene. *Nature* **386**: 451–452.

Wang H, Zhou Y, Bird DA, Fowke LC. 2008. Functions, regulation and cellular localization of plant cyclin-dependent kinase inhibitors. *Journal of Microscopy* **231**: 234–246.

Wang H, Zhou Y, Gilmer S, Whitwill S, Fowke LC. 2000. Expression of the plant cyclin-dependent kinase inhibitor ICK1 affects cell division, plant growth and morphology. *Plant Journal* **24**: 613–623.

Weinl C, Marquardt S, Kuijt SJ, Nowack MK, Jacoby MJ, Hülskamp M, Schnittger A. 2005. Novel functions of plant cyclin-dependent kinase inhibitors, ICK1/KRP1, can act non-cell-autonomously and inhibit entry into mitosis. *The Plant Cell* **17**: 1704–1722.

Wiggers RJ, Starr JL, Price HJ. 1990. DNA content and variation in chromosome number in plant cells affected by *Meloidogyne incognita* and *M. arenaria*. *Phytopathology* **80**: 1391–1395.

Zhou Y, Fowke LC, Wang H. 2002. Plant CDK inhibitors: studies of interactions with cell cycle regulators in the yeast two-hybrid system and functional comparisons in transgenic *Arabidopsis* plants. *Plant Cell Reports* **20**: 967–975.

Supporting Information

Additional supporting information may be found in the online version of this article.

Fig. S1 Expression patterns in uninfected roots of seven *KRPpro:GUS* Arabidopsis lines.

Fig. S2 Expression patterns in whole-mount galls of seven *KRPpro:GUS* Arabidopsis lines.

Fig. S3 Expression patterns of *KRP1pro:GUS*, *KRP3pro:GUS*, *KRP4pro:GUS* and *KRP7pro:GUS* Arabidopsis lines during gall development.

Fig. S4 *In situ* localization of *KRP1*, *KRP3*, *KRP4* and *KRP7* mRNAs in Arabidopsis roots infected with *M. incognita*.

Fig. S5 Characterization of *krp* loss-of-function lines.

Fig. S6 Mitotic images are often seen in giant cells of the *krp2* line.

Fig. S7 Nematode infection tests of *krp* loss-of-function lines compared with wild type.

Fig. S8 Plant morphology of *KRP* overexpression lines used for *M. incognita* inoculation assays.

Fig. S9 Electron micrographs of galls of the $KRP2^{OE}$ line and Arabidopsis wild-type plants.

Fig. S10 Nuclear flow cytometry analyses of uninfected roots in wild type, $KRP1^{OE}$ and $KRP2^{OE}$ lines.

Fig. S11 KRP1-GFP and free-GFP protein expression during gall development.

Table S1 List of primers

Table S2 Summary of expression patterns of seven *KRPpro:GUS* Arabidopsis lines during gall development

Movie S1 3D confocal projections of serial optical sections of a 30-d-old gall induced by *M. incognita* in Arabidopsis wild-type roots.

Movie S2 3D confocal projections of serial optical sections of a 40-d-old gall induced by *M. incognita* in the $KRP1^{OE}$ line.

Movie S3 3D confocal projections of serial optical sections of a 40-d-old gall induced by *M. incognita* in the $KRP2^{OE}$ line.

Movie S4 GFP-KRP2 expression in tobacco BY2 cells during cell division.

Movie S5 GFP-KRP2 protein level is regulated by the root-knot nematode during gall development.

Please note: Wiley-Blackwell are not responsible for the content or functionality of any supporting information supplied by the authors. Any queries (other than missing material) should be directed to the *New Phytologist* Central Office.